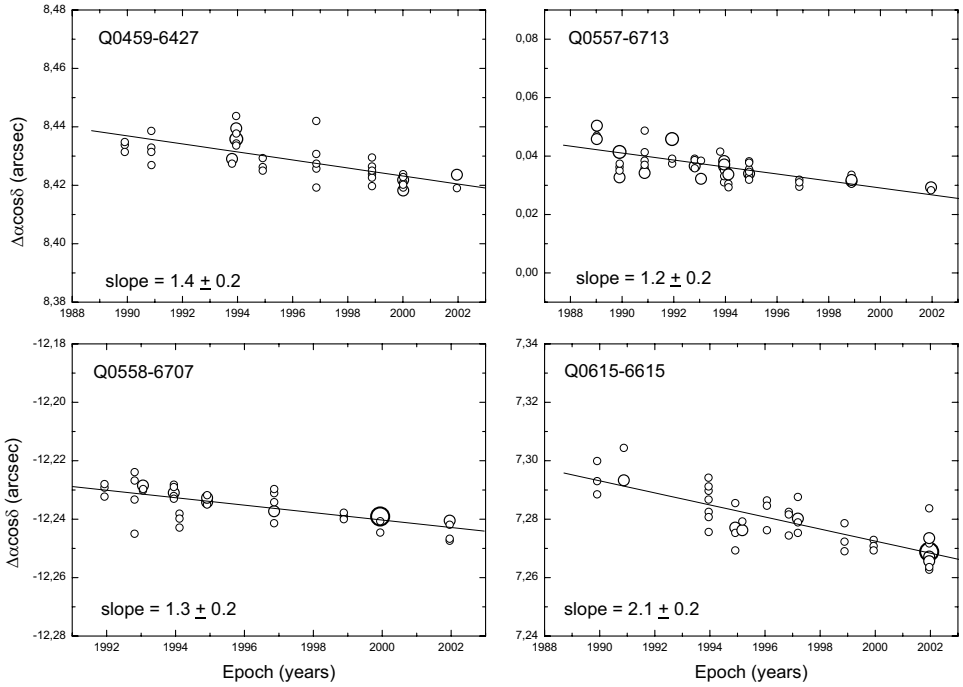

Fig. 2. Relative positions in R.A. ($\Delta\alpha\cos\delta$) vs. epoch of observation for the studied fields. The values of $\Delta\alpha\cos\delta$ represent the individual positions of the QSO on different CCD frames relative to the barycenter of the SRF. The point sizes are proportional to the number of times the measurement yielded the same coordinate value for a particular epoch (extra-small, small, medium, large and extra-large sizes indicate one to five measurements per epoch, respectively). The best-fit straight lines from linear regression analyses on the data are also shown.

in R.A., and ±0.26 (±0.52), ±0.60 (±0.71), ±0.36 (±0.58), ±0.26 (±0.62) mas yr^{-1} in DEC, for Q0459-6427, Q0557-6713, Q0558-6707 and Q0615-6615, respectively.

We believe the improvement is mainly due to the new third degree polynomial registration process used in the present work. It seems that the latter is quite adequate for the optics of the telescope we used, which, by the way, was never changed throughout the entire time baseline of this project. As stated in PCM06, we believe the scatter shown in the plots probably stems entirely from the random errors in the measurements and the registration process, and does not represent the actual velocity dispersion in the LMC.

In Figures 2 and 3 we present position vs. epoch diagrams for the QSO fields in R.A. ($\Delta\alpha\cos\delta$) and DEC ($\Delta\delta$), where $\Delta\alpha\cos\delta$ and $\Delta\delta$ represent the (X, Y) positions of the QSO on different CCD frames, relative to the barycenter of the SRF. These diagrams were obtained using individual position data for the QSO in each CCD image as a function of epoch. In Table 3 we give the mean barycentric positions of the QSOs per epoch, along with their mean errors (the errors of the averages). The heading N (sixth column) represents the sum of all data points (one per image) used to calculate the mean for each coordinate and corresponding epoch (first column). This sum is the same for both R.A. and DEC. Also shown (last column) are the CCD detectors used in each epoch. Symbol sizes in Figures 2 and 3 are proportional to the number of times the measurements yielded the same coordinate value for a particular epoch. The latter may be different for R.A. and DEC, since each point in Figures 2 and 3 represents a subset of data points in a small range of coordinates; thus, the number of points in the range may be different for R.A. and DEC, but the sum af all the points for a particular epoch is the same for both coordinates, as shown in Table 3. This is done to avoid point overlapping in the graph. The best-fit straight lines resulting from simple linear regression analysis on the data points are also shown. The negative values of the line slopes correspond to the PM of the barycenter of the LRS in each QSO field.

Table 4 summarizes our results for the (measured) PM of the LMC. Column 1 gives the quasar identification, Columns 2 and 3 the R.A. and DEC components (together with their standard deviations) of the LMC PM,